CORE
Metadata, citation and similar papers at core.ac.uk
Provided by Open Archive Toulouse Archive Ouverte

A Predictive Control With Flying Capacitor Balancing of a Multicell Active Power Filter

François Defaÿ, Ana-Maria Llor, *Member, IEEE*, and Maurice Fadel, *Member, IEEE*

***Abstract*—Unlike traditional inverters, multicell inverters have the following advantages: lower switching frequency, high number of output levels, and less voltage constraints on the insulated-gate bipolar transistors. Significant performances are provided with this structure which is constituted with flying capacitors. This paper deals with a predictive and direct control applied to the multicell inverter for an original application of this converter: a three-phase active filter. To take advantage of the capabilities of the multicell converter in terms of redundant control states, a voltage control method of flying capacitor is added, based on the use of a switching table. Flying capacitor voltages are kept on a fixed interval, and precise voltage sensors are not necessary. The association of predictive control and voltage balancing increases considerably the bandwidth of the active filter.**

***Index Terms*—Active power filter, flying capacitor, multicell inverter, switching table.**

I. Introduction

In RECENT years, industrial applications and uses of multicell inverters, also called flying capacitor inverters (locomotive, modular design, low inductance busbars, etc.), have increased [1], [2]. In addition, active power filters have been performed [3], and different devices and control methods have been tested to improve the bandwidth of classical inverters (pulsewidth modulation, hysteresis, and dead-beat control) [4]–[9]. Pure active power filters are more expensive than hybrid active power filters, but they assume more functions than passive or hybrid active filters [10]. Multilevel inverters are more and more used for active power filter [11], [12], and the use of multicell inverters increases [13]. The use of multicell inverters, which benefit from several advantages such as low switching ripple, few conduction losses, and small dV/dt, is a way to improve the bandwidth of active power filters [14]. Multicell inverters have as particularity to be constituted with flying capacitors. These capacitors have to be balanced to guarantee the good voltage value at the output [15]. The balancing of flying capacitors can be made naturally, but the control of inverter would not be optimal from a current control point of view [16]. To perform the control of the inverter, considering that voltage balancing and current regulation do not have the same bandwidth, a control on several switching periods is allowed for flying capacitors. It consists to impose a trend of variation to each flying capacitor on several periods of control. This paper proposes a new method to control the balancing of flying capacitors coupled with a predictive control of current in a composed voltage frame. Predictive control is more and more used for the current control of classical inverters [17] and multilevel inverters [18], [19]. In this paper, a predictive controller is applied to a multicell inverter for an active filter operation based on the repetitive principle of current reference. The voltage balancing repose on the control of tendency is applied to each flying capacitor. This method requires only the detection of flying capacitor voltage compared with a threshold, which corresponds only to a binary value and does not require accurate voltage probes or voltage observers [20]. In consequence, the bandwidth of the multicell inverter is increased [21].

TABLE I
CONFIGURATION AND CAPACITOR VOLTAGE TENDENCY FOR A THREE-CELL INVERTER

Configuration: $C_i : [S_{c_{i3}}\ S_{c_{i2}}\ S_{c_{i1}}]$	Level: $N_i * E/3$	$i_{ch_i} > 0$		$i_{ch_i} < 0$	
		v_{ci1}	v_{ci2}	v_{ci1}	v_{ci2}
0 : [0 0 0]	0	⇝	⇝	⇝	⇝
1 : [0 0 1]	$E/3$	↘	⇝	↗	⇝
2 : [0 1 0]	$E/3$	↗	↘	↘	↗
3 : [0 1 1]	$2 * E/3$	⇝	↘	⇝	↗
4 : [1 0 0]	$E/3$	⇝	↗	⇝	↘
5 : [1 0 1]	$2 * E/3$	↘	↗	↗	↘
6 : [1 1 0]	$2 * E/3$	↗	⇝	↘	⇝
7 : [1 1 1]	E	⇝	⇝	⇝	⇝

II. Model of the Multicell Active Power Filter

A. Definitions

Level—N_i: It is the instantaneous level of voltage at the output of the inverter (for the phase i). N_i can take four values for a three-cell inverter: 0, 1, 2, and 3 [cf. Fig. 4(top)] with $i = A, B, C$.

Configuration—C_i: It represents the instantaneous output voltage state of the inverter, which is represented by the state of each commutation cell. Table I presents the eight possible configurations for a three-cell multicellular inverter. Fig. 1 shows the configuration 4 [1 0 0] of the inverter. The function state $S_{c_{ij}} = 1$ corresponds to a closed insulated-gate bipolar transistor (IGBT).

Manuscript received February 21, 2008; revised June 16, 2008. First published July 9, 2008; last published August 29, 2008 (projected).

F. Defaÿ and A.-M. Llor are with the LAPLACE Laboratory, Université de Toulouse, 31071 Toulouse, France (e-mail: defay@laplace.univ-tlse.fr; llor@laplace.univ-tlse.fr).

M. Fadel is with the LAPLACE Laboratory, Université de Toulouse, 31071 Toulouse, France, and also with the École Nationale Supérieure d'Électrotechnique, d'Électronique, d'Informatique, d'Hydraulique, et des Télécommunications, 31071 Toulouse Cedex 7, France (e-mail: fadel@laplace.univ-tlse.fr).

Color versions of one or more of the figures in this paper are available online at http://ieeexplore.ieee.org.

Digital Object Identifier 10.1109/TIE.2008.927989

0278-0046/$25.00 © 2008 IEEE

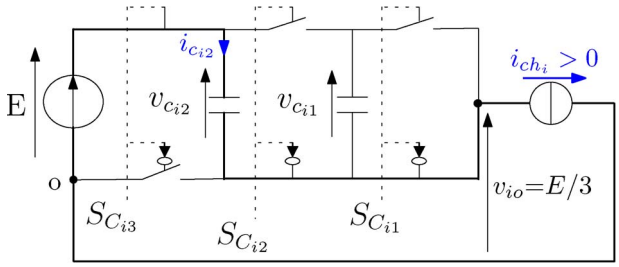

Fig. 1. Configuration ($C_i = 4$) for a three-cell inverter.

B. Model in the Composed Voltage Frame (ba-ca Frame)

Fig. 2 shows a three-cell inverter connected to an R, L, E charge, which is representative of an active filtering function. Active filter is connected to an electric network; thus, load voltages ($V_{\rm an}$, $V_{\rm bn}$, and $V_{\rm cn}$) will be considered as perturbations. Their measurement or their estimation is made to compensate their effects.

If flying capacitor voltages are constant, the output voltage of phase i, designed as $V_{i\rm O}$, can be expressed as [15]

$$V_{i\rm O} = \frac{E}{3} * (N_i), \qquad \text{with } i = A, B, C. \tag{1}$$

Output voltage can be expressed in the composed voltage frame (ba-ca frame) considering that $V_{AB} = V_{A\rm O} - V_{B\rm O}$

$$\begin{cases} V_{AB} = \frac{E}{3} * (N_A - N_B) \\ V_{BC} = \frac{E}{3} * (N_B - N_C). \end{cases} \tag{2}$$

The use of this ba-ca frame allows control of the current with only two voltage references because the use of composed voltages guarantees the good balancing of the system (cf. Fig. 3). This frame is particularly adapted for active power filters because the state variables are directly accessible without any transformations and the neutral point of the network, which is sometimes not accessible, is not needed. Moreover, in this frame, three variables ($N_A, N_B,$ and N_C) are used to control only two state variables (V_{AB} and V_{BC}) (2). In Fig. 4, the average voltage value at the time instant t_k ($\overline{V_{i\rm O}^k}$) is shown and can be expressed as a function of $\overline{N_i^k}$, which represents the average voltage value on a period T_d.

$\overline{N_i^k}$ can take continuous values between zero and three and is comparable to the duty cycle of a classical inverter. The system is described as follows:

$$\begin{pmatrix} \overline{V_{AB}^k} \\ \overline{V_{BC}^k} \end{pmatrix} = \frac{E}{3} * \begin{pmatrix} 1 & -1 & 0 \\ 0 & 1 & -1 \end{pmatrix} * \begin{pmatrix} \overline{N_A^k} \\ \overline{N_B^k} \\ \overline{N_C^k} \end{pmatrix} = \frac{E}{3} * M * \begin{pmatrix} \overline{N_A^k} \\ \overline{N_B^k} \\ \overline{N_C^k} \end{pmatrix}. \tag{3}$$

It is a classical problem of least squares.

Variables i_{AB} and i_{BC} are introduced as $(i_{\rm ch_1} - i_{\rm ch_2})$ and $(i_{\rm ch_2} - i_{\rm ch_3})$, respectively,

$$\begin{cases} \frac{d(i_{AB})}{dt} = -\frac{r_{\rm ch}}{l_{\rm ch}} * (i_{AB}) + \frac{1}{l_{\rm ch}} * v_{AB} - \frac{1}{l_{\rm ch}} * v_{ab} \\ \frac{d(i_{BC})}{dt} = -\frac{r_{\rm ch}}{l_{\rm ch}} * (i_{BC}) + \frac{1}{l_{\rm ch}} * v_{BC} - \frac{1}{l_{\rm ch}} * v_{bc}. \end{cases} \tag{4}$$

Equation (4) can be expressed as a classical continuous state-space system: $\dot{X} = A * X + B * U$ with

$$\begin{cases} X = \begin{pmatrix} i_{AB} \\ i_{BC} \end{pmatrix}, & U = \begin{pmatrix} v_{AB} - v_{ab} \\ v_{BC} - v_{bc} \end{pmatrix} \\ A = \begin{pmatrix} -\frac{r_{\rm ch}}{l_{\rm ch}} & 0 \\ 0 & -\frac{r_{\rm ch}}{l_{\rm ch}} \end{pmatrix}, & B = \begin{pmatrix} \frac{1}{l_{\rm ch}} & 0 \\ 0 & \frac{1}{l_{\rm ch}} \end{pmatrix}. \end{cases} \tag{5}$$

This system is discretized considering that the switching period T_d is the same as the sampling period. The state matrix A of the continuous state space is diagonal; thus, the discretization is simple

$$\begin{pmatrix} i_{AB}^{k+1} \\ i_{BC}^{k+1} \end{pmatrix} = A_k * \begin{pmatrix} i_{AB}^k \\ i_{BC}^k \end{pmatrix} + B_k * \begin{pmatrix} v_{AB}^k - v_{ab}^k \\ v_{BC}^k - v_{bc}^k \end{pmatrix} \tag{6}$$

with

$$\begin{cases} A_k = e^{A * T_{\rm d}} \\ B_k = A^{-1} * (e^{A * T_{\rm d}} - I) * B \end{cases} \tag{7}$$

where I is the identity matrix with the appropriate dimension.

III. Application for an Active Power Filter

To improve the bandwidth of the active power filter, a direct predictive control will be applied. It consists to calculate the switching control action of the next switching period during the actual period. This control requires balanced flying capacitor voltages and is completely discrete, based on (6). The direct predictive control system of the active filter is shown in Fig. 5 and is composed of four main blocs.

1) **Calculation of the harmonic currents:** The method of the instantaneous active and reactive powers [22] is used on the ba-ca frame. On this frame, the principle of the method does not change as long as no neutral point is connected the network. In the case of unbalanced network voltage, the harmonics extraction is not efficient as in a classical frame [23].
2) **Prediction of reference current and network voltage:** Current value is obtained using the repetitive reference principle coupled to a simple interpolation. It consists to record the reference on time interval and use the recorded value to make a projection at the time instant t_{k+2}. Voltage is easily predicted considering that the network is regulated.
3) **Calculation of the average inverter output voltage for the next switching period:** To obtain a powerful control law, a predictive control can be applied to the inverter. Equation (6) can be inverted to obtain the required average output for the next switching period. The recurrence obtained is given as follows:

$$\begin{pmatrix} v_{AB}^{k+1} \\ v_{BC}^{k+1} \end{pmatrix} = K_1 * \begin{pmatrix} i_{AB}^{k+2} \\ i_{BC}^{k+2} \end{pmatrix} + K_2 * \begin{pmatrix} i_{AB}^k \\ i_{BC}^k \end{pmatrix} + \begin{pmatrix} v_{ab}^{k+1} \\ v_{bc}^{k+1} \end{pmatrix} + K_3 * \begin{pmatrix} v_{AB}^k - v_{ab}^k \\ v_{BC}^k - v_{bc}^k \end{pmatrix} \tag{8}$$

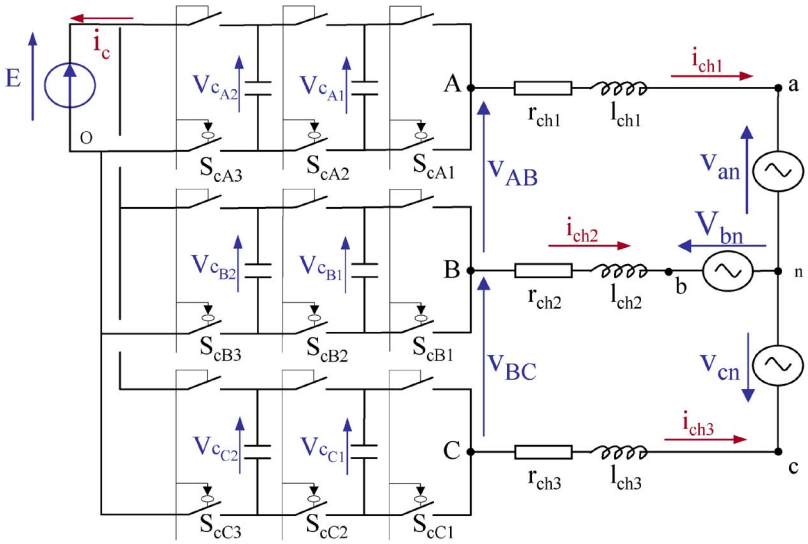

Fig. 2. Flying capacitor inverters with the R, L, E charge.

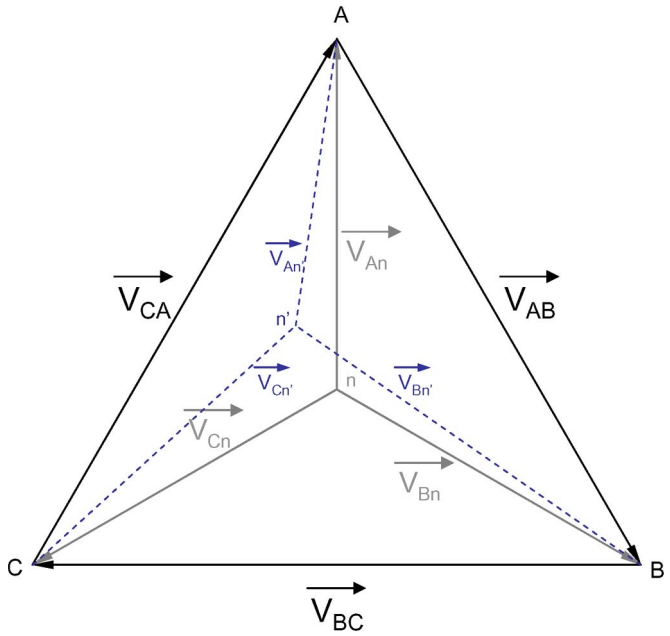

Fig. 3. Vectorial voltage diagram.

with

$$\begin{cases} K_1 = B_k^{-1} \\ K_2 = -B_k^{-1} * A_k^2 \\ K_3 = -B_k^{-1} * A_k * B_k. \end{cases}$$

References needed at the time instants (t_{k+1} and t_{k+2}) will be given, owing to the repetitive reference principle 2). At each switching time, (8) gives the next average voltage which has to be applied at the output of the inverter. An output solution is obtained, and the calculation of the switching orders can be made to respect the flying capacitor balancing. Equation (3) is an underdetermined problem of least squares. To find the solution, a singular value decomposition is used to calculate the pseudoinverse $M^{\dagger}$ of the matrix M [24] expressed in (3)

$$\begin{pmatrix} \overline{N_1^{k+1}} \\ \overline{N_2^{k+1}} \\ \overline{N_3^{k+1}} \end{pmatrix} = M^{\dagger} * \begin{pmatrix} \overline{V_{AB}^{k+1}} \\ \overline{V_{BC}^{k+1}} \end{pmatrix} \qquad M^{\dagger} = \frac{3}{E} * \begin{pmatrix} 2/3 & 1/3 \\ -1/3 & 1/3 \\ -1/3 & -2/3 \end{pmatrix}. \tag{9}$$

4) **Balancing of flying capacitor and dc capacitor:** The principle of flying capacitor balancing with appropriate profile selection is exposed in the next section. The dc bus is regulated by injecting an active component of the current reference.

IV. Balancing Flying Capacitor on an Interval of Voltage

A. Definitions

Profile—P_i: The profile applied to the phase i is composed by the sequence of four configurations. It is defined for one switching period (T_d). To create profiles, the switching period is divided in a hundred intervals. It allows good precision on the output voltage value and easy programming with a field-programmable gate array (FPGA). Fig. 6 shows two different profiles which are defined by four configurations (C_{i1}, C_{i2}, C_{i3}, and C_{i4}), four application times (t_1, t_2, t_3, and t_4), and four corresponding output level voltages (N_{i1}, N_{i2}, N_{i3}, and N_{i4}). One profile is then defined as

$$P_i = \begin{cases} (C_{i1}, C_{i2}, C_{i3}, C_{i4}) \\ (t_{i1}, t_{i2}, t_{i3}, t_{i4}) \\ (N_{i1}, N_{i2}, N_{i3}, N_{i4}). \end{cases}$$

The average voltage at the output for one switching period is expressed as

$$\overline{V_{iO}} = \frac{1}{T_d} * (t_1 * N_{i1} + t_2 * N_{i2} + t_3 * N_{i3} + t_4 * N_{i4}). \tag{10}$$

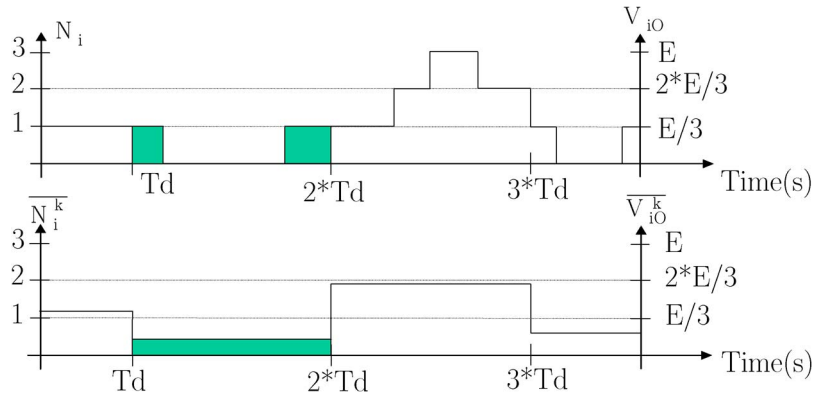

Fig. 4. Representation of the output voltage.

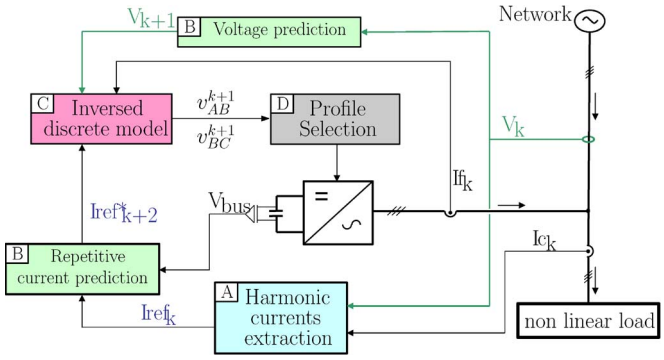

Fig. 5. Description of control operations.

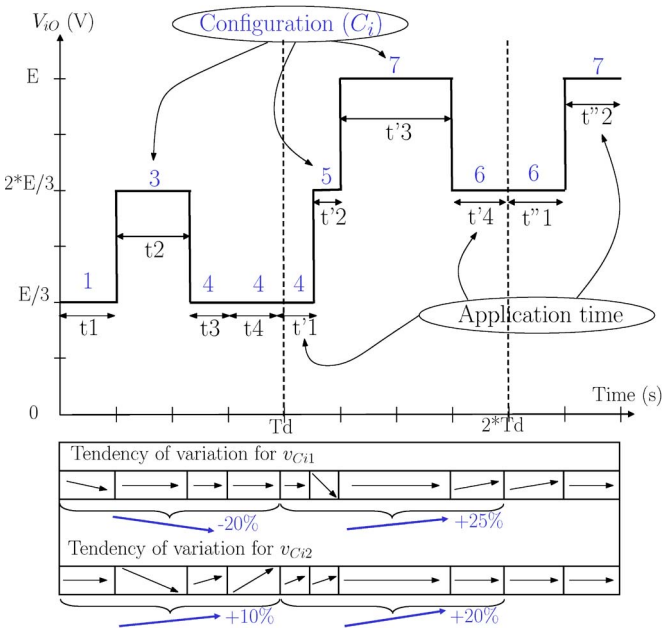

Fig. 6. Example of two profiles.

State—E_i: This is a variable which represents the state of the multicell inverter (and not its configuration) related to the instantaneous current. In fact, this state will be useful for the choice of the profile to be applied.

Two binary variables are introduced to define Table II. First, sign_i represents the sign of the output current such as "$\text{sign}_i = 1$" if "$I_{\text{ch}_i} > 0$" and "$\text{sign}_i = 0$" if "$I_{\text{ch}_i} < 0$," respectively. Second, $T_{Vc_{ij}}$ represents the tendency of variation that will be given to the flying capacitor voltage Vc_{ij}. It has been chosen that "$T_{Vc_{ij}} = 0$" corresponds to the decrease of Vc_{ij} and that "$T_{Vc_{ij}} = 1$" corresponds to the increase of Vc_{ij}. The tendency is determined by the comparison of voltage with a threshold. An analogical comparison gives a numerical information which represents the value of $T_{Vc_{ij}}$. No analog-to-digital converter (ADC) is required to control one flying capacitor voltage but only a digital bit.

TABLE II
STATE OF THE THREE-PHASE MULTICELL INVERTER

$sign_i$	0	0	0	0	1	1	1	1
$T_{Vc_{i2}}$	0	0	1	1	0	0	1	1
$T_{Vc_{i1}}$	0	1	0	1	0	1	0	1
E_i	0	1	2	3	4	5	6	7

B. Principle

On a multicell inverter, the flying capacitor current is directly proportional to the control signals of the commutation cells on each side of the capacitor

$$I_{C_{ij}} = (S_{c_{ij+1}} - S_{c_{ij}}) * I_{\text{ch}_i}. \tag{11}$$

The current predictive controller calculates the three control actions (average voltages for the next switching period) with the use of (8) and (3). On the example shown in Fig. 7, the average voltage value 1.5 can be applied with different means, due to the fact that different levels are available at the output of the inverter.

In fact, the important thing is to assure the good average value. The effect of applying E during 1/2 period and zero during the rest of the period is the same as that of applying $2E/3$ during the first 1/2 period and $E/3$ during the second 1/2 period. However, the configuration which is applied on the inverter has an influence on the current of flying capacitor (11), thus an influence on the voltage.

Table I gives the variations of flying capacitors corresponding to each configuration. For each average level at the output, there are different profiles available. Fig. 8 shows some profile examples starting with the same level (0). Different profiles can be applied to assure one average level, but they do not have the same effects on each flying capacitor (cf. Fig. 6).

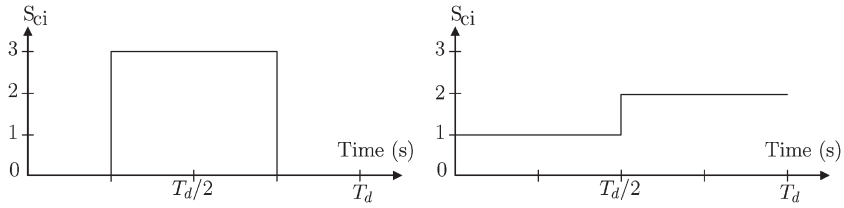

Fig. 7. Two examples to obtain $E/2$.

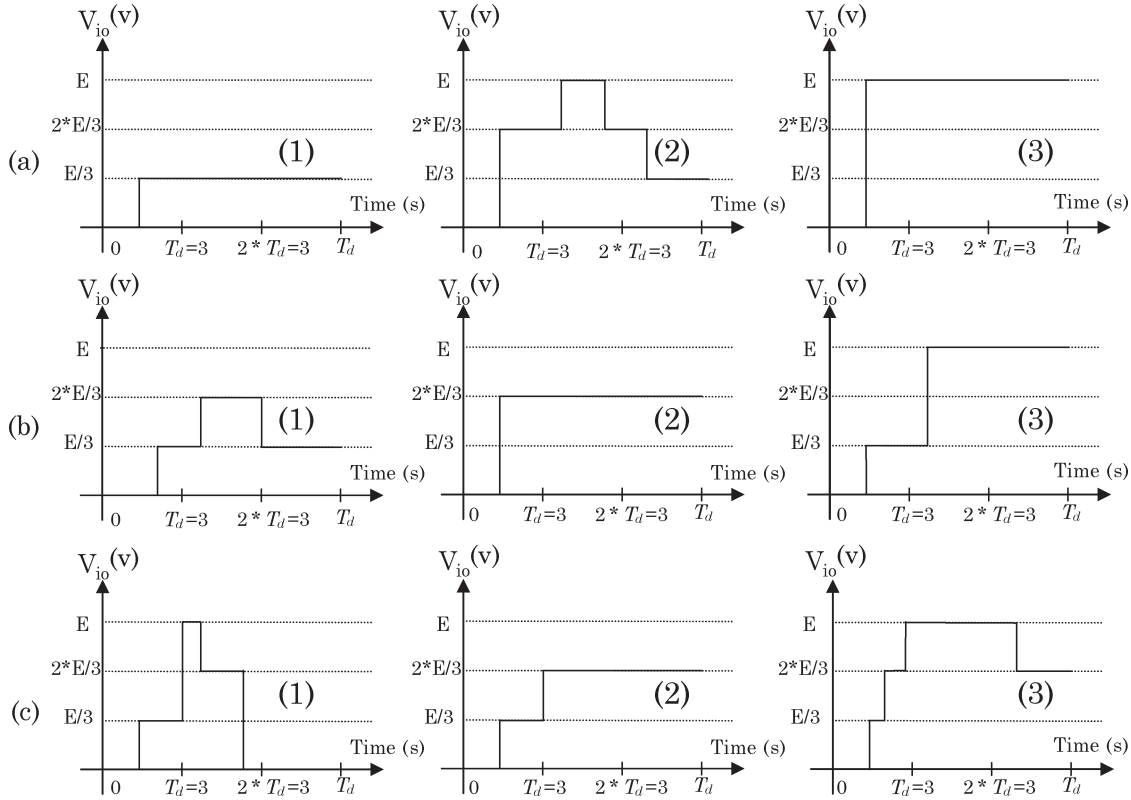

Fig. 8. Different profiles available starting from level 0.

C. Switching Table

The main idea is to achieve the balancing of flying capacitor with the use of switching tables (calculated offline) to guarantee a good computing time for practical implementation. For its definition, some constraints must be respected.

1) Strong level transitions are not allowed (output voltage transitions of more than $E/3$ are forbidden).
2) Initial and final levels can take only two values ($E/3$ or $2E/3$).
3) The number of level changes is limited to three on a switching period in order to reduce the number of possible profiles. In addition, it allows division of the switching frequency by two on the IGBT because only one state change is allowed during one switching period.

To respect these constraints, the profile table contains, as an input parameter, the previous profile to avoid brutal transitions and to indicate the starting level of the new profile, which corresponds to the fourth level of the old profile. Based on the state of the inverter, the desired level of voltage, and the

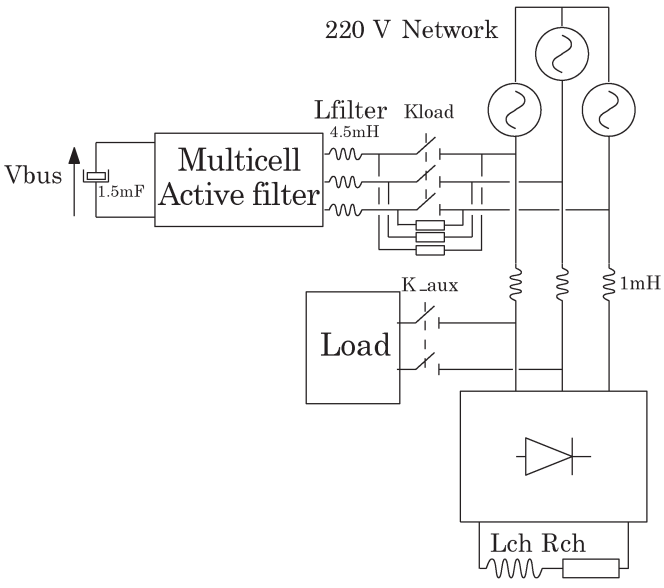

Fig. 9. Configuration of electrical circuit with active filter.

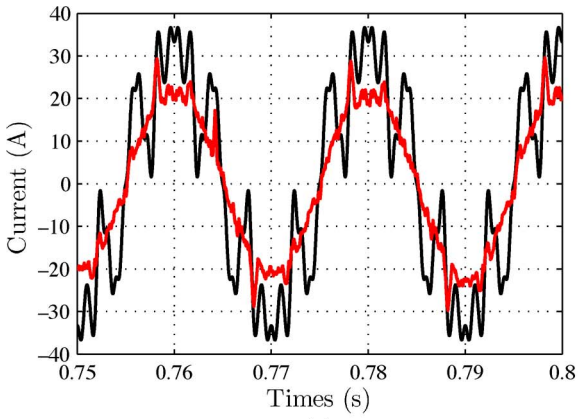

(a)

	I_{load} (A)	$I_{network}$	
		C=200 μF	C=400 μF
I_{fond}	15	15.3	15.15
I_{h5}	8.2	0.37	0.4
I_{h7}	4.5	0.38	0.36
I_{h11}	1.2	0.12	0.12
I_{h13}	0.9	0.35	0.37
I_{h17}	0.3	0.21	0.2
I_{h19}	0.75	0.37	0.31
I_{h23}	0.3	0.38	0.33
I_{h25}	3	1.2	1.2
I_{h29}	0	0.33	0.32
THD	44.5%	1.1%	1.15%

(b)

Fig. 10. Currents of phase A for a strong level harmonics load.

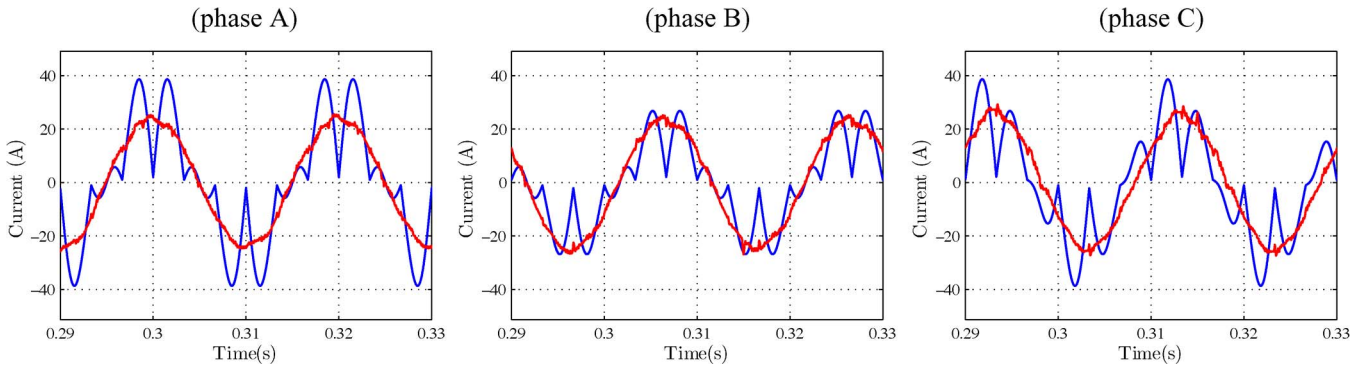

Fig. 11. Unbalanced current of the load and the network.

previous configuration, it can be found that the best profile to apply is that which contains the four configurations and the four application times. This table has been generated automatically with an adapted algorithm. It is important to note that this table is fixed and calculated offline, which constitutes an additional advantage. A table for a higher number of levels can be generated automatically.

V. Simulation Results

The flying capacitor control has been extensively tested in simulation, including current prediction models, the discrete reverse model, the choice of commutations, and the sampling of variables. Simulations are made with an instantaneous model of an active power filter. Fig. 9 shows the electrical configuration with the principal parameters. Other parameters are a 2.5-kHz switching frequency, a 600-V dc bus, and a 10-kV · A load.

A. Results for a Strong Level Harmonics Load

To demonstrate the excellent bandwidth of the filter, a current load is added to increase the 25th-harmonic level to 3 A. Fig. 10(a) shows the active filter operation on a strong level harmonics load. The 25th-harmonic level is considerably decreased (from 3 to 1.2 A) with a switching frequency of the filter of only 2.5 kHz. Moreover, the total harmonic distortion (THD) is considerably decreased from 45% to 1.2% with this predictive control of multicell active filter.

TABLE III
THD Analysis of Each Phase

	phase	I_{load}	$I_{network}$	
			C=200μF	C=400μF
I_{fond}	A	19A	16.1A	16.2A
THD		21.2%	0.22%	0.21%
I_{fond}	B	13.3A	16.2A	16.2A
THD		18.9%	0.22%	0.22%
I_{fond}	C	16.5A	16.4A	16.3A
THD		21%	0.26%	0.25%

B. Results for an Unbalanced Load

To test the effectiveness of the presented control method, a test is made with an unbalanced load. The load and the network currents are given in Fig. 11 which shows the good filtering and balancing operation. The analysis (cf. Table III) of current amplitude and THD of the three phases shows that the value of flying capacitors has no real influence. This control method allows correct control of the current.

C. Voltage Balancing

Fig. 12(a) and (b) shows the variation of flying capacitor voltages and the dc-bus for two different values of flying capacitors. Three perturbations are introduced: one at the time 0.02 s (start of the active filtering function), one at the time 0.2 s (which is due to the first load variation), and one at the time 0.6 s (load variation and unbalanced current).

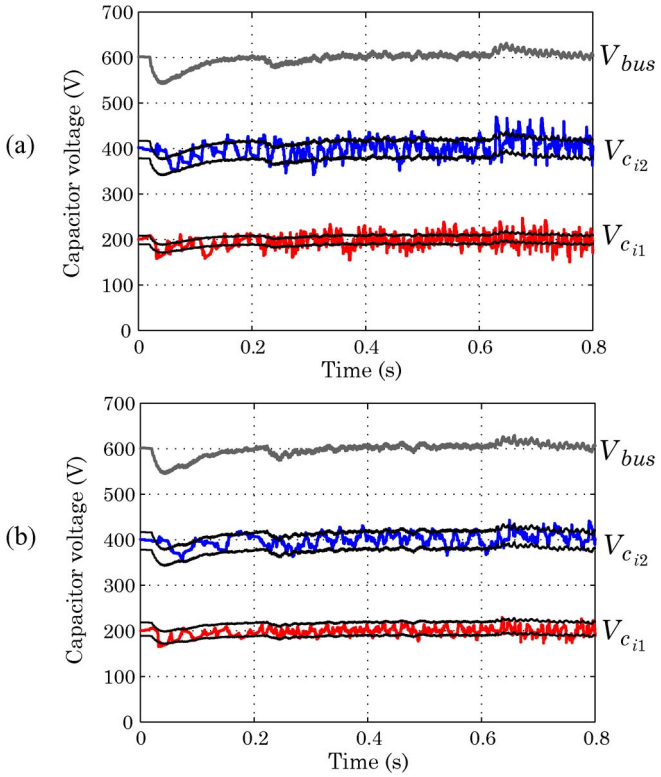

Fig. 12. Flying capacitors and dc-bus voltages of (a) 200 μF and (b) 400 μF.

The flying capacitor voltages are well kept in the interval of $\pm 5\%$ for a 4000-μF flying capacitor and are slightly out of the interval for a lower flying capacitor value. Voltage balancing is accomplished considering that the switching frequency (2.5 kHz) is low and that the harmonic current content (more than the 25th harmonics) is important. Moreover, the value of the flying capacitor has an effect on the voltage ripple but has no real influence neither on the current control nor on the THD (cf. Fig. 10). These results validate the control on an interval of voltage which allows increase of the bandwidth of the multicell inverter.

VI. Experimental Results

Experimental results have been carried out with the experimental test bench shown in Fig. 13. It is composed of a multicellular inverter that is able to work with a 1800-V dc bus and a 600-A line current.

The presented results are obtained for a 220-V network. A three-phase diode rectifier load is proposed for the balanced and unbalanced tests. The principal characteristics of the operating system are as follows:

1) a three-phase multicell inverter with 18 IGBTs;
2) a Dspace DS1105 controller with 16 fast ADCs;
3) an Altera FPGA for protection and IGBT control;
4) a 1.5-mF capacitor for dc bus;
5) three 4.5-mH inductors for the filtering operation;
6) six flying capacitors of 200 μF.

The current of the balanced load is shown in Fig. 14; it corresponds to a diode rectifier classical form which presents a THD of 23%. Three experiments have been carried out at different switching frequencies: 10, 5, and 2.5 kHz [Fig. 15(a)–(c)]. The THDs of the network current are of 2.2%, 2.6%, and 2.7%, respectively, after the filtering operation. The current ripple increases when the switching frequency decreases, but the current regulation is correct. This is due to the value of the filter inductors which are constant on each case.

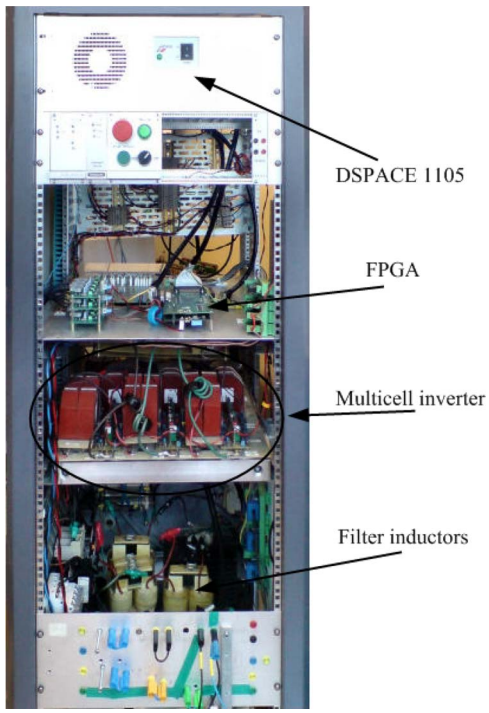

Fig. 13. Experimental bench.

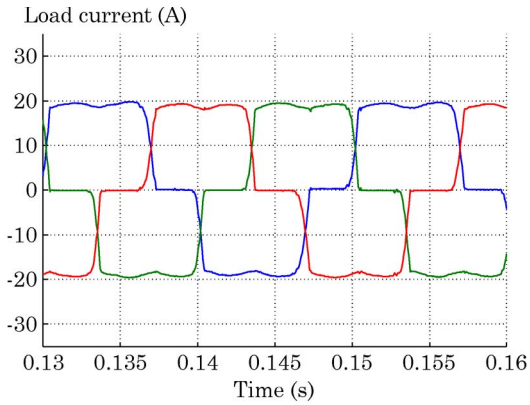

Fig. 14. Load currents.

The cases of 5 and 2.5 kHz are really similar, which shows the excellent bandwidth of the multicell inverter used for the active filtering operation. Concerning the voltage balancing of the flying capacitors, results are better than in simulation. Fig. 16 shows the voltage balancing for a 2.5-kHz switching frequency and proves the efficiency of the switching tables. The interval of variation is less than 5% of the nominal voltage value. The value of the flying capacitor is ten times lower than the dc bus, and this value can be reduced by two with the use of the tables.

Another experiment has been done concerning an unbalanced load which has been created with the superposition of a

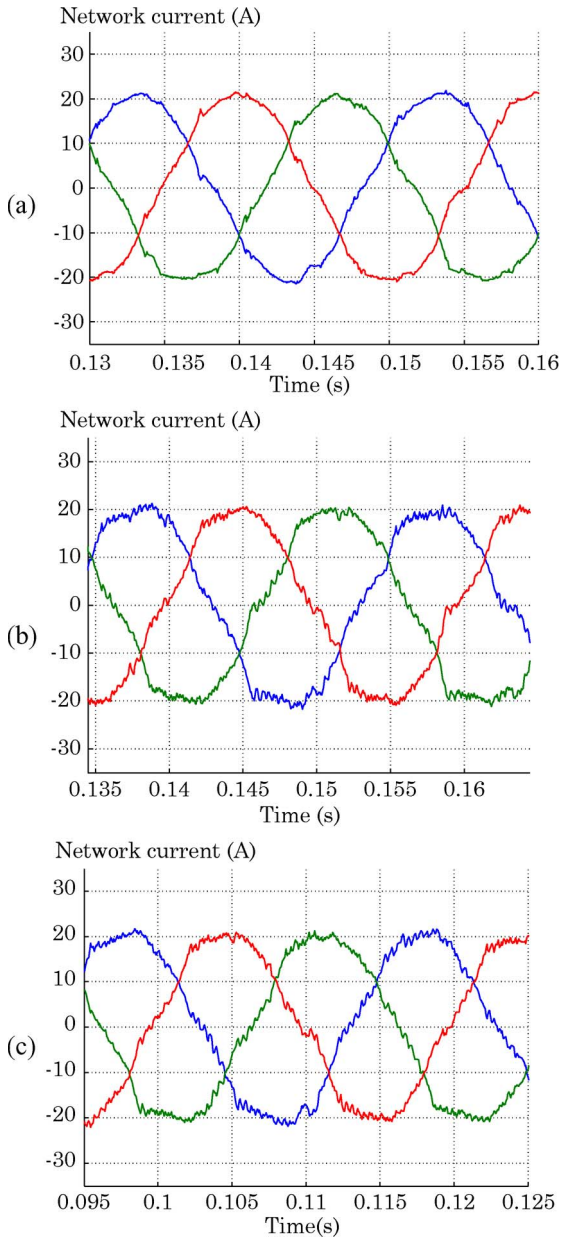

Fig. 15. Network currents for different switching frequency values.

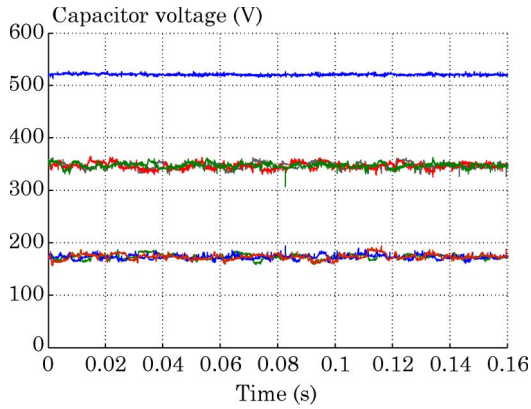

Fig. 16. Voltage balancing for a 2.5-kHz switching frequency.

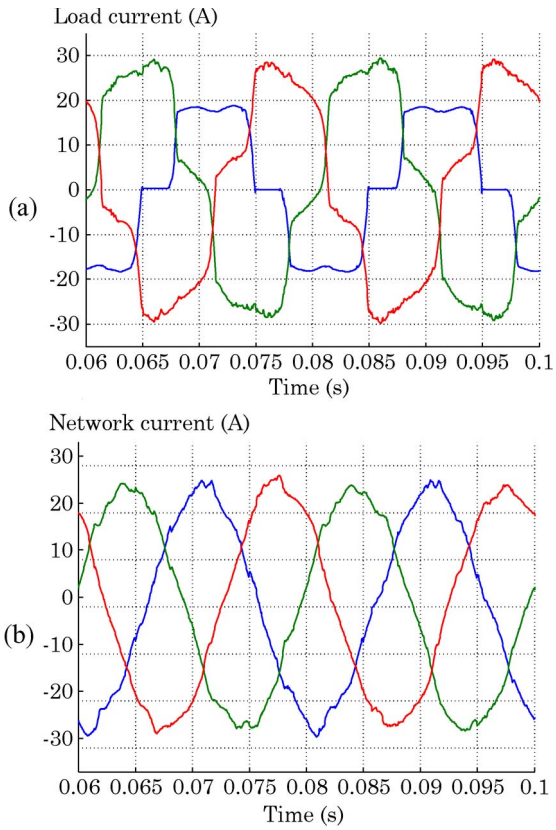

Fig. 17. Unbalanced (a) load and (b) network currents.

single-phase load (the K_aux contactor (Fig. 9) is switched on). The network currents are well balanced, as shown in Fig. 17(b).

The performance of the multicell active filter has been established. The experimental THD is a bit more important than in the simulation, which seems normal. In the experimental work, noise and current ripple effects appear on the current measurement and need to be treated in future experiments.

Compared with the neutral point clamped (NPC) multilevel inverters, multicell is attractive for medium voltage applications if the carrier frequency is higher than 1000 Hz [25], [26] because the cost of flying capacitor is reduced. For active filtering, this frequency is generally more important to reduce harmonics. Moreover, it is very complicated to control an NPC device with more than three levels compared with the multicell inverters.

VII. Conclusion

The bandwidth of the active filter is considerably increased compared with a classic inverter due to the use of a multicell inverter combined with a predictive control.

Experimental results for a diode rectifier load show that the THD of network current is reduced to 2.7% with a 2.5-kHz switching frequency. Results for an unbalanced load show the capabilities of the control in the proposed ba-ca frame.

The balancing of the flying capacitor voltages, which is rather independent of the current regulation, allows them to benefit from the four output voltage levels without depending on the voltage regulation. This control needs only one binary information for each flying capacitor and no more sensors than a classical active filter.

Moreover, the use of switching tables, calculated offline, presents the advantage of not requiring an important computing time. Finally, it allows the predictive control to be independent of the delay control time because the instants of commutation are calculated for the next switching period.

REFERENCES

[1] T. Meynard, H. Foch, P. Thomas, J. Courault, R. Jacob, and M. Nahrstaedt, "Multicell converters: Basic concepts and industry applications," *IEEE Trans. Ind. Electron.*, vol. 49, no. 5, pp. 955–964, Oct. 2002.

[2] D. Krug, M. Malinowski, and S. Bernet, "Design and comparison of medium voltage multi-level converters for industry applications," in *Conf. Rec. 39th IEEE IAS Annu. Meeting*, 2004, vol. 2, pp. 781–790.

[3] H. Akagi, "Active harmonic filters," *Proc. IEEE*, vol. 93, no. 12, pp. 2128–2140, Dec. 2005.

[4] M. Routimo, M. Salo, and H. Tuusa, "Comparison of voltage-source and current-source shunt active power filters," in *Proc. IEEE Power Electron. Spec. Conf.*, 2005, pp. 2571–2577.

[5] J. Mossoba and P. Lehn, "A controller architecture for high bandwidth active power filters," *IEEE Trans. Power Electron.*, vol. 18, no. 1, pp. 317–325, Jan. 2003.

[6] T. Green and J. Marks, "Control techniques for active power filters," *Proc. Inst. Elect. Eng.—Electr. Power Appl.*, vol. 152, no. 2, pp. 369–381, Mar. 2005.

[7] R. Grino, R. Cardoner, R. Costa-Castello, and E. Fossas, "Digital repetitive control of a three-phase four-wire shunt active filter," *IEEE Trans. Ind. Electron.*, vol. 54, no. 3, pp. 1495–1503, Jun. 2007.

[8] P. Parkatti, M. Salo, and H. Tuusa, "A novel vector controlled current source shunt active power filter with reduced component voltage stresses," in *Proc. IEEE PESC*, Jun. 17–21, 2007, pp. 1121–1125.

[9] J. Allmeling, "A control structure for fast harmonics compensation in active filters," *IEEE Trans. Power Electron.*, vol. 19, no. 2, pp. 508–514, Mar. 2004.

[10] Y. Tamai, S. Srianthumrong, and H. Akagi, "Comparisons between a hybrid shunt active filter and a pure shunt active filter," *Elect. Eng. Jpn.*, vol. 153, no. 2, pp. 61–70, 2005.

[11] G. Zhou, B. Wu, and D. Xu, "Direct power control of a multilevel inverter based active power filter," *Electr. Power Syst. Res.*, vol. 77, no. 3/4, pp. 284–294, Mar. 2007.

[12] B.-R. Lin and T.-Y. Yang, "Three-level voltage-source inverter for shunt active filter," *Proc. Inst. Electr. Eng.—Electr. Power Appl.*, vol. 151, no. 6, pp. 744–751, Nov. 7, 2004. filtrage.

[13] B.-R. Lin and C.-H. Huang, "Implementation of a three-phase capacitor-clamped active power filter under unbalanced condition," *IEEE Trans. Ind. Electron.*, vol. 53, no. 5, pp. 1621–1630, Oct. 2006.

[14] C. Martins, X. Roboam, T. Meynard, and A. Carvalho, "Switching frequency imposition and ripple reduction in DTC drives by using a multilevel converter," *IEEE Trans. Power Electron.*, vol. 17, no. 2, pp. 286–297, Mar. 2002.

[15] T. Meynard, M. Fadel, and N. Aouda, "Modeling of multilevel converters," *IEEE Trans. Ind. Electron.*, vol. 44, no. 3, pp. 356–364, Jun. 1997.

[16] A. Donzel and G. Bornard, "New control law for capacitor voltage balance in multilevel inverter with switching rate control (CVC)," in *Conf. Rec. IEEE IAS Annu. Meeting*, 2000, pp. 2037–2044.

[17] J. Rodriguez, J. Pontt, C. A. Silva, P. Correa, P. Lezana, P. Cortes, and U. Ammann, "Predictive current control of a voltage source inverter," *IEEE Trans. Ind. Electron.*, vol. 54, no. 1, pp. 495–503, Feb. 2007.

[18] P. Zanchetta, D. B. Gerry, V. G. Monopoli, J. C. Clare, and P. W. Wheeler, "Predictive current control for multilevel active rectifiers with reduced switching frequency," *IEEE Trans. Ind. Electron.*, vol. 55, no. 1, pp. 163–172, Jan. 2008.

[19] R. Vargas, P. Cortes, U. Ammann, J. Rodriguez, and J. Pontt, "Predictive control of a three-phase neutral-point-clamped inverter," *IEEE Trans. Ind. Electron.*, vol. 54, no. 5, pp. 2697–2705, Oct. 2007.

[20] A.-M. Lienhardt, G. Gateau, and T. Meynard, "Digital sliding-mode observer implementation using FPGA," *IEEE Trans. Ind. Electron.*, vol. 54, no. 4, pp. 1865–1875, Aug. 2007.

[21] F. Defay, A. Llor, and M. Fadel, "An active power filter using a sensorless muticell inverter," in *Proc. IEEE ISIE*, Jun. 4–7, 2007, pp. 679–684.

[22] F. Peng and J. Lai, "Generalized instantaneous reactive power theory for three-phase power systems," *IEEE Trans. Instrum. Meas.*, vol. 45, no. 1, pp. 293–297, Feb. 1996.

[23] R. S. Herrera, P. Salmerón, and H. Kim, "Instantaneous reactive power theory applied to active power filter compensation: Different approaches, assessment, and experimental results," *IEEE Trans. Ind. Electron.*, vol. 55, no. 1, pp. 184–196, Jan. 2008.

[24] F. Defay, A. M. Llor, and M. Fadel, "A direct predictive control of shunt active power filters using multicell converter," in *Proc. Eur. Conf. Power Electron. Appl.*, Sep. 2–5, 2007, pp. 1–9.

[25] J. Rodriguez, S. Bernet, B. Wu, J. Pontt, and S. Kouro, "Multilevel voltage-source-converter topologies for industrial medium-voltage drives," *IEEE Trans. Ind. Electron.*, vol. 54, no. 6, pp. 2930–2945, Dec. 2007.

[26] D. Krug, S. Bernet, S. Fazel, K. Jalili, and M. Malinowski, "Comparison of 2.3-kV medium-voltage multilevel converters for industrial medium-voltage drives," *IEEE Trans. Ind. Electron.*, vol. 54, no. 6, pp. 2979–2992, Dec. 2007.

François Defaÿ was born in 1980. He received the B.S. degree in electrical engineering from the Institut National Polytechnique de Grenoble, Grenoble, France, in 2003, and the M.S. degree from the Institut National Polytechnique de Toulouse, Toulouse, France, in 2005. He is currently working toward the Ph.D. degree in the LAPLACE Laboratory, Universite de Toulouse, Toulouse.

Ana-Maria Llor (M'08) received the M.S. degree from the Escuela Politecnica Superior de la Universidad Carlos III, Madrid, Spain, in 1998, and the Ph.D. degree from the Escuela Politecnica Superior de la Universidad Carlos III, Madrid, and the Institut National des Sciences Appliquees, Lyon, France, in 2003.

Since 2005, she has been an Assistant Professor with the LAPLACE Laboratory (formerly Laboratoire d'Electrotechnique et d'Electronique Industrielle until January 2007), Université de Toulouse, Toulouse, France. Her research interests include hybrid control of power converters, digital control of electrical systems, and multilevel converters.

Maurice Fadel (M'08) received the Ph.D. degree from the Institut National Polytechnique de Toulouse, Toulouse, France, in 1988.

Since 1985, he has been with the LAPLACE Laboratory (formerly Laboratoire d'Electrotechnique et d'Electronique Industrielle), Universite de Toulouse, Toulouse. His work concerns the modeling and control of electric systems. He is currently the Deputy Director of LAPLACE. This laboratory is composed of 200 researchers in the field of plasma and energy conversion. He is also currently a Professor with the École Nationale Superieure d'Électrotechnique, d'Électronique, d'Informatique, d'Hydraulique, et des Télécommunications, Toulouse. He has authored numerous published technical papers in the field of multicell converter control and sensorless permanent-magnet synchronous motors (PMSMs).